

Vision Guided Navigation for a Nonholonomic Mobile Robot

Yi Ma, *Student Member, IEEE*, Jana Košecká, and Shankar S. Sastry, *Fellow, IEEE*

Abstract—Visual servoing, i.e., the use of the vision sensor in feedback control, has gained recently increased attention from researchers both in vision and control community. A fair amount of work has been done in applications in autonomous driving, manipulation, mobile robot navigation and surveillance. However, theoretical and analytical aspects of the problem have not received much attention. Furthermore, the problem of estimation from the vision measurements has been considered separately from the design of the control strategies. Instead of addressing the pose estimation and control problems separately, we attempt to characterize the types of control tasks which can be achieved using only quantities directly measurable in the image, bypassing the pose estimation phase. We consider the task of navigation for a nonholonomic ground mobile base tracking an arbitrarily shaped continuous ground curve. This tracking problem is formulated as one of controlling the shape of the curve in the image plane. We study the controllability of the system characterizing the dynamics of the image curve, and show that the shape of the image curve is controllable only up to its “linear” curvature parameters. We present stabilizing control laws for tracking piecewise analytic curves, and propose to track arbitrary curves by approximating them by piecewise “linear” curvature curves. Simulation results are given for these control schemes. Observability of the curve dynamics by using direct measurements from vision sensors as the outputs is studied and an Extended Kalman Filter is proposed to dynamically estimate the image quantities needed for feedback control from the actual noisy images.

Index Terms—Mobile robots, trajectory tracking, visual servoing.

I. INTRODUCTION

SENSING of the environment and subsequent control are important features of the navigation of an autonomous mobile agent. In spite of the fact that there has been an increased interest in the use of visual servoing in the control loop, sensing and control problems have usually been studied separately. The literature in computer vision has mainly concentrated on the process of estimating necessary information about the state of the agent in the environment and the structure of the environment, e.g., [1]–[4], while control issues have been often addressed separately. On the other hand, control approaches typically assume the full specification of

the environment and task as well as the availability of the state estimate of the agent.

The dynamic vision approach proposed by Dickmanns, Mysliwetz, and Graefe [5]–[7] makes the connection between the estimation and control tighter by setting up a dynamic model of the evolution of the curvature of the road in a driving application. Curvature estimates are used only for the estimation of the state of the vehicle with respect to the road frame in which the control objective is formulated or for the feedforward component of the control law. Control for steering along a curved road directly using the measurement of the projection of the road tangent and its optical flow has been previously considered by Raviv and Herman [8]. However, stability and robustness issues have not yet been addressed, and no statements have been made as to what extent these cues are sufficient for general road scenarios. A visual servoing framework proposed in [9] and [10] by Espiau *et al.* and Samson *et al.* addresses control issues directly in the image plane and outlines the dynamics of certain simple geometric primitives. Further extensions of this approach for nonholonomic mobile platforms has been made by Pissard-Gibollet and Rives [11]. Generalization of the curve tracking and estimation problem outlined in Dickmanns to arbitrarily shaped curves addressing both the estimation of the shape parameters as well as control has been explored in [12] by Frezza and Picci. They used an approximation of an arbitrary curve by a spline, and proposed a scheme for recursive estimation of the shape parameters of the curve, and designed control laws for tracking the curve.

For a theoretical treatment of the problem, a general understanding of the dynamics of the image of an arbitrary ground curve is crucial. Therefore in this paper, before we specify particular control objectives (such as point-stabilization or trajectory tracking), we first study general properties of dynamic systems associated with image curves. Authors in [13] formulated the problem of tracking as that of controlling the shape of the ground curve in the image plane. In spite of the fact that the system characterizing the image curve is in general infinite-dimensional, we show that for linear curvature curves the system is finite dimensional. When the control problem is formulated as one of controlling the image curve dynamics, we prove that the controllability distribution has dimension 3 and show that the system characterizing the image curve dynamics is fully controllable only up to the linear curvature term regardless of the kinematics of the mobile robot base. It is also shown that linear curvature curve has finite dimensional

Manuscript received December 4, 1997; revised February 16, 1998. This paper was recommended for publication by Associate Editor S. Hutchinson and Editor V. Lumelsky upon evaluation of the reviewers' comments. This work was supported by ARO under MURI Grant DAAH04-96-1-0341.

The authors are with the Electronics Research Laboratory, University of California, Berkeley, CA 94720-1774 USA.

Publisher Item Identifier S 1042-296X(99)04179-8.

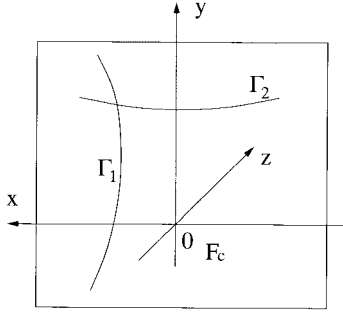


Fig. 3. Example showing that a ground curve Γ_2 cannot be parameterized by y , while the curve Γ_1 can be.

the unicycle model and then extend it to the bicycle model capturing the kinematics of the car.

B. Image Curve Dynamics Analysis

In this section, we consider a planar curve Γ on the ground, and study how the shape of the image of the curve Γ evolves under the motion of the mobile robot. For the rest of this paper, we make the following assumptions:

Assumption 1: The ground curve Γ is an analytic curve, i.e., Γ can be locally represented by its convergent Taylor series expansion.

Assumption 2: The ground curve Γ is such that it can be parameterized by y in the camera coordinate frame F_c .

Assumption 2 guarantees that the task of tracking the curve Γ can be solved using a smooth control law. For example, if the curve is orthogonal to the direction of the heading of the mobile robot, such as the curve Γ_2 shown in Fig. 3, it can not be parameterized by y . Obviously, in this case, if the mobile robot needs to track the curve Γ_2 , it has to make a decision as to the direction for tracking the curve: turning right or turning left. This decision cannot be made using smooth control laws [20].

1) *Relations between Orthographic and Perspective Projections:* According to Assumption 2, at any time t , the curve Γ can be expressed in the camera coordinate frame as $(\gamma_x(y, t), y, \gamma_z(y, t))^T \in \mathbb{R}^3$. Since Γ is a planar curve on the ground, $\gamma_z(y, t)$ is given by

$$\gamma_z(y, t) = \frac{d + y \cos \phi}{\sin \phi} \quad (3)$$

which is a function of only y . Thus only $\gamma_x(y, t)$ changes with time and determines the dynamics of the ground curve. In order to determine the dynamics of the image curve we consider both *orthographic* and *perspective* projection and show that under certain conditions they are equivalent.

The orthographic projection image curve of Γ in the image plane $z = 1$ given by $(\gamma_x(y, t), y)^T \in \mathbb{R}^2$ is denoted by $\tilde{\Gamma}$, as shown in Fig. 4.

On the other hand, the perspective projection image curve, denoted by Λ , is given in the image plane coordinates by

$$\begin{aligned} X(y, t) &= \frac{\gamma_x}{\gamma_z} = \frac{\gamma_x(y, t) \sin \phi}{d + y \cos \phi} \\ Y(y, t) &= \frac{y}{\gamma_z} = \frac{y \sin \phi}{d + y \cos \phi}. \end{aligned} \quad (4)$$

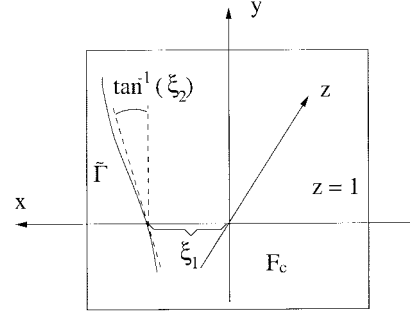


Fig. 4. The orthographic projection of a ground curve on the $z = 1$ plane. Here $\xi_1 = \gamma_x$ and $\xi_2 = (\partial \gamma_x / \partial y)$.

Note in (4) that $Y(y, t)$ is a function of y alone and that the derivative of $Y(y, t)$ with respect to y is given by $(\partial Y(y, t) / \partial y) = (d \sin \phi / (d + y \cos \phi)^2) > 0$ so long as $\phi > 0$ and $y \neq -d / \cos \phi$. Using the inverse function theorem, locally, the image curve Λ can be re-parameterized by Y when $(\partial Y(y, t) / \partial y) \neq 0$. Λ can then be represented by $(\lambda_X(Y, t), Y)^T \in \mathbb{R}^2$ in the image plane coordinates, where the function $\lambda_X(Y, t)$ can be directly measured. However, since, as we will soon see, for the given ground curve Γ , it is easier to get an explicit expression for the dynamics of its orthographic image $\tilde{\Gamma}$ than the perspective projection image Λ . Thus, it will be helpful to find the relation between these two image curves $\tilde{\Gamma}$ and Λ , i.e., the relations between the two functions γ_x and λ_X . First, let us simplify the notation. Define

$$\begin{aligned} \xi_{i+1} &\equiv \frac{\partial^i \gamma_x(y, t)}{\partial y^i}, \quad \zeta_{i+1} \equiv \frac{\partial^i \lambda_X(Y, t)}{\partial Y^i} \\ \xi^i &\equiv (\xi_1, \xi_2, \dots, \xi_i)^T \in \mathbb{R}^i, \quad \xi \equiv \xi^\infty \\ \zeta^i &\equiv (\zeta_1, \zeta_2, \dots, \zeta_i)^T \in \mathbb{R}^i, \quad \zeta \equiv \zeta^\infty. \end{aligned}$$

If $\gamma_x(y, t)$ is an analytic function of y , $\gamma_x(y, t)$ is completely determined by the vector ξ evaluated at any y ; similarly for $\lambda_X(Y, t)$. Thus, the relations between $\tilde{\Gamma}$ and Λ are given by the relations between ξ and ζ for the case of analytic curves.

Lemma 1: (Equivalence of ξ , ζ Coordinates)

Consider the orthographic projection image curve $\tilde{\Gamma} = (\gamma_x(y, t), y)^T$ and the perspective projection image curve $\Lambda = (\lambda_X(Y, t), Y)^T$, with ξ and ζ defined in (5). Assume that the tilt angle $\phi > 0$ and $y \neq -d / \cos \phi$. Then for any fixed y , $\zeta^n = A_n(y) \xi^n, \forall n \in \mathbb{N}$, where $A_n(y) \in \mathbb{R}^{n \times n}$ is a nonsingular lower triangular matrix.

Proof: We prove this lemma by using mathematical induction. For $n = 1$, from (4), $\zeta^1 = (\sin \phi / d + y \cos \phi) \xi^1$, so that the lemma is true for $n = 1$. Now suppose that the lemma is true for all $n \leq k$, i.e.

$$\zeta^n = A_n(y) \xi^n, \quad n = 1, 2, \dots, k \quad (5)$$

where all $A_n(y)$ are nonsingular lower triangular matrices. Clearly, in order to prove that for $n = k + 1$ the lemma is still true, it suffices to prove that ζ_{k+1} is a linear combination of ξ^{k+1} , i.e.

$$\zeta_{k+1} = \sum_{i=1}^{k+1} \beta_i(y) \xi_i. \quad (6)$$

Since $A_{k+1}(y)$ is nonsingular, $\beta_{k+1}(y)$ needs to be nonzero. Differentiating (5) with respect to y , we have

$$\begin{aligned} \frac{\partial \zeta^k}{\partial Y} \frac{\partial Y(y, t)}{\partial y} &= A'_k(y) \xi^k + A_k(y) \frac{\partial \xi^k}{\partial y} \\ \Rightarrow \frac{\partial \zeta^k}{\partial Y} &= \frac{A'_k(y)}{\frac{\partial Y(y, t)}{\partial y}} \xi^k + \frac{A_k(y)}{\frac{\partial Y(y, t)}{\partial y}} \frac{\partial \xi^k}{\partial y} \end{aligned} \quad (7)$$

where the last entry of the column vector $\partial \zeta^k / \partial Y$ is ζ_{k+1} and

$$\frac{\partial \xi^k}{\partial y} = (\xi_2, \xi_3, \dots, \xi_{k+1})^T. \quad (8)$$

Therefore, according to (7), ζ_{k+1} is a linear combination of ξ^{k+1} and, since $A_k(y)$ is a $k \times k$ nonsingular lower triangular matrix, $A_k(y)_{kk} \neq 0$,² the coefficient $\beta_{k+1}(y) = (A_k(y)_{kk} / (\partial Y(y, t) / \partial y))$ is nonzero. ■

Example: We calculate the matrix $A_4(y) \in \mathbb{R}^{4 \times 4}$ to be (9), shown at the bottom of this page.

Lemma 1 tells us that under certain conditions, the dynamics of the system ξ for the orthographic projection image curve and that of ζ for the perspective projection image curve are algebraically equivalent. We may obtain either one of them from the other. ζ are quantities that we can directly measure from the perspective projection image Λ . Our ultimate goal is to design feedback control laws exclusively using these image quantities. However, as we will soon see, it is much easier to analyze the curve's dynamics in terms of ξ , the quantities in the orthographic projection image. It also turns out to be easier to design feedback control laws in terms of ξ . For these reasons, in the following sections, we choose system ξ (i.e., the orthographic projection image) for studying our problem and design control laws since it simplifies the notation.

2) *Dynamics of General Analytic Curves:* While the mobile robot moves, a point attached to the spatial frame F_f moves in the opposite direction relative to the camera frame F_c . Thus, from (2), for points on the ground curve $\Gamma = (\gamma_x(y, t), y, \gamma_z(y))^T$, we have

$$\dot{\gamma}_x(y, t) = -(y \sin \phi + \gamma_z \cos \phi) \omega. \quad (10)$$

Also, by chain rule

$$\begin{aligned} \dot{\gamma}_x(y, t) &= \frac{\partial \gamma_x}{\partial t} + \frac{\partial \gamma_x}{\partial y} \dot{y} \\ &= \frac{\partial \gamma_x}{\partial t} + \frac{\partial \gamma_x}{\partial y} (-(v \sin \phi - \gamma_x \omega \sin \phi)). \end{aligned} \quad (11)$$

² $A_k(y)_{kk}$ is the (k, k) entry of the matrix $A_k(y)$.

The shape of the orthographic projection of the ground curve $\tilde{\Gamma} = (\gamma_x(y, t), y)^T$ then evolves in the image plane $z = 1$ according to the following *Riccati-type* partial differential equation:³

$$\frac{\partial \gamma_x}{\partial t} = -(y \sin \phi + \gamma_z \cos \phi) \omega + \frac{\partial \gamma_x}{\partial y} (v - \gamma_x \omega) \sin \phi. \quad (12)$$

Using the notation ξ from (5) and the expression (3) for γ_z , this partial differential equation can be transformed to an infinite-dimensional dynamic system ξ through differentiating equation (12) with respect to y repeatedly

$$\dot{\xi} = f_1 \omega + f_2 v \quad (13)$$

where $f_1 \in \mathbb{R}^\infty$ and $f_2 \in \mathbb{R}^\infty$ are

$$\begin{aligned} f_1 &= - \begin{bmatrix} \xi_1 \xi_2 \sin \phi + d \cot \phi + \frac{y}{\sin \phi} \\ \xi_1 \xi_3 \sin \phi + \xi_2^2 \sin \phi + \frac{1}{\sin \phi} \\ \xi_1 \xi_4 \sin \phi + 3 \xi_2 \xi_3 \sin \phi \\ \vdots \\ \xi_1 \xi_{i+1} \sin \phi + g_i(\xi_2, \dots, \xi_i) \\ \vdots \end{bmatrix} \\ f_2 &= \begin{bmatrix} \xi_2 \sin \phi \\ \xi_3 \sin \phi \\ \xi_4 \sin \phi \\ \vdots \\ \xi_{i+1} \sin \phi \\ \vdots \end{bmatrix} \end{aligned}$$

where $g_i(\xi_2, \dots, \xi_i)$ are appropriate functions (polynomials) of only ξ_2, \dots, ξ_i . In the general case, the system (13) is an infinite-dimensional system.

It may be argued that the projective or orthographic projections induce a diffeomorphism (so-called homography, in the vision literature [21] between the ground plane and the image plane. Thus, we could write an equation of the form (13) for the dynamics of the mobile robot following a curve in the coordinate frame of the ground plane. These could be equivalent to the curve dynamics (13) described in the image plane through the push forward of the homography. We have not taken this point of view for reasons that we explain in Section III.

³ This equation is called a Riccati-type PDE since it generalizes the classical well-known Riccati equation for the motion of a homogeneous straight line under rotation around the origin [12], [11].

$$\begin{bmatrix} \frac{\sin \phi}{d + y \cos \phi} & 0 & 0 & 0 \\ -\frac{\cos \phi}{d} & \frac{d + y \cos \phi}{d} & 0 & 0 \\ 0 & 0 & \frac{(d + y \cos \phi)^3}{d^2 \sin \phi} & 0 \\ 0 & 0 & 3 \frac{(d + y \cos \phi)^4 \cos \phi}{d^3 \sin^2 \phi} & \frac{(d + y \cos \phi)^5}{d^3 \sin^2 \phi} \end{bmatrix} \quad (9)$$

3) *Dynamics of Linear Curvature Curves:* In this section, we consider a special case when the ground planar curve Γ is a *linear curvature curve*, such that the derivative of its curvature $k(s)$ with respect to the arc-length parameter s is a nonzero constant, i.e., $k'(s) \equiv c \neq 0$. These curves are also referred to as *clothoids*. If $k'(s) \equiv 0$, the curve is just a *constant curvature curve* which is a degenerate case of linear curvature curves. Note that, according to this definition, both straight lines and circles are constant curvature curves, but not linear curvature curves. Constant curvature curves may be regarded as degenerate cases of linear curvature curves. For linear curvature curves, we have the following lemma.

Lemma 2: For a ground curve Γ of linear curvature, i.e., $k'(s) \equiv c \neq 0$, for any $i \geq 4$, ξ_i can be expressed as a function of ξ_1, ξ_2 , and ξ_3 alone.

Proof: Consider the ground curve $\Gamma = (\gamma_x(y, t), y, \gamma_z(y, t))^T$ where $\gamma_z(y, t)$ is given in (3). For the arc-length parameter s and the curvature k , the following relationships hold:

$$s'(y) = \sqrt{\left(\frac{\partial \gamma_x}{\partial y}\right)^2 + 1 + \left(\frac{\partial \gamma_z}{\partial y}\right)^2} \quad (14)$$

$$k(y) = \frac{\|\Gamma'(y) \times \Gamma''(y)\|_2}{s'(y)^3} = \frac{a \frac{\partial^2 \gamma_x}{\partial y^2}}{\left(\sqrt{a^2 + \left(\frac{\partial \gamma_x}{\partial y}\right)^2}\right)^3} \quad (15)$$

where a is defined as $a \equiv \sqrt{1 + \cot^2 \phi} = (\sin \phi)^{-1}$. Thus the derivative of the curvature k with respect to the arc-length parameter s is given by

$$\begin{aligned} k'(s) &= \frac{k'(y)}{s'(y)} \\ &= a \frac{\frac{\partial^3 \gamma_x}{\partial y^3} \left(a^2 + \left(\frac{\partial \gamma_x}{\partial y}\right)^2\right) - 3 \frac{\partial \gamma_x}{\partial y} \left(\frac{\partial^2 \gamma_x}{\partial y^2}\right)^2}{\left(a^2 + \left(\frac{\partial \gamma_x}{\partial y}\right)^2\right)^3}. \end{aligned} \quad (16)$$

Using the definition of ξ_i , from (16) ξ_4 can be expressed by

$$\xi_4 = \frac{c(a^2 + \xi_2^2)^3/a + 3\xi_2\xi_3^2}{a^2 + \xi_2^2}. \quad (17)$$

Therefore, ξ_4 is a function of ξ_1, ξ_2 , and ξ_3 alone. According to the definition of ξ_i , it follows that, for all $i > 4$, ξ_i are functions of ξ_1, ξ_2 , and ξ_3 only. ■

Using Lemma 2, for a ground linear curvature curve Γ , the dynamics of its orthographic projection image $\tilde{\Gamma}$, i.e., system (13) for ξ , can then be simplified to be the following three-dimensional (3-D) system $\xi^3 = (\xi_1, \xi_2, \xi_3)^T$

$$\dot{\xi}^3 = f_1^3 \omega + f_2^3 v \quad (18)$$

where $f_1^3 \in \mathbb{R}^3$ and $f_2^3 \in \mathbb{R}^3$ are

$$\begin{aligned} f_1^3 &= - \begin{bmatrix} \xi_2 \xi_1 \sin \phi + d \cot \phi + \frac{y}{\sin \phi} \\ \xi_3 \xi_1 \sin \phi + \xi_2^2 \sin \phi + \frac{1}{\sin \phi} \\ \xi_4 \xi_1 \sin \phi + 3\xi_2 \xi_3 \sin \phi \end{bmatrix} \\ f_2^3 &= \begin{bmatrix} \xi_2 \sin \phi \\ \xi_3 \sin \phi \\ \xi_4 \sin \phi \end{bmatrix} \end{aligned} \quad (19)$$

where ξ_4 is given by (17).

Combining Lemma 1 and Lemma 2, we have the following remark:

Remark 1: For a ground curve of linear curvature, the dynamics of ζ for the perspective projection image of the curve are completely determined by three independent states $\zeta_1, \zeta_2, \zeta_3$, or equivalently, for $i \geq 4$, ζ_i is a function of only ζ_1, ζ_2 , and ζ_3 . The two systems $\zeta^3 = (\zeta_1, \zeta_2, \zeta_3)^T$ and $\xi^3 = (\xi_1, \xi_2, \xi_3)^T$ are equivalent and related by equation (9). This implies, for instance, that these two systems have the same controllability properties.

In the case that Γ is a constant curvature curve, i.e., $k'(s) \equiv 0$, one can show that ξ_3 is actually a function of only ξ_1, ξ_2 , so for all $\xi_i, i > 3$ are functions of only ξ_1, ξ_2 . There are then only two independent states ξ_1, ξ_2 for the dynamics of system ξ .

Linear curvature is an *intrinsic property* (which is preserved under Euclidean motions i.e., $SE(2)$) of planar curves. Thus, the expression (17) always holds under all planar motions of the robot. However, some other seemingly natural and simple assumptions that the literature has taken for the ground curve (so as to simplify the problem) might fail to be preserved under the robot's motions. For example, if, in order to simplify (13), one assumes $\xi_i = 0$ for $i \geq 4$, i.e., $\gamma_x(y, t)$ is of the form

$$\gamma_x(y, t) = \xi_1(y_0, t) + \xi_2(y_0, t)(y - y_0) + \frac{1}{2}\xi_3(y_0, t)(y - y_0)^2.$$

This property is not preserved under rotations. More generally, it is not an intrinsic property for a planar curve that its Taylor series expansion has a finite number of terms. Therefore, one cannot simplify system (13) to a finite-dimensional system by assuming that the curve's Taylor series expansion is finite (which may be the case only at special positions).⁴

III. CONTROLLABILITY ISSUES

We are interested in being able to control the shape of the image curves. From the above discussion, this problem is equivalent to the problem of controlling system ξ (13) in the unicycle case. For linear curvature curves, the infinite-dimensional system ξ is reduced to the 3-D system ξ^3 (18). In this section, we study the controllability of such systems. If the systems characterizing the curve Γ are controllable, that essentially means that given our control inputs we can steer the mobile base in order to achieve desired position and shape of the curve in the image plane.

Once again, using the homography between the image plane and the ground plane the controllability could be studied on

⁴Essentially, it only "simplifies" the initial conditions of the system (13), not the system dimension.

the ground plane alone. We have chosen not to do so for the following reasons.

- 1) We want to use vision as a image based servoing sensor in the control loop. Studying the ground plane curve dynamics alone does not give the sort of explicit control laws that we will obtain.
- 2) We agree that, due the homography between the image plane and the ground plane, for certain control tasks, it is indeed equivalent to design the control in the cartesian space or in the image space. But, by lifting the dynamics onto the image plane, one will be able to clearly classify the type of control tasks which can be achieved through feedback from the image quantities. The controllability and observability issues of such tasks can then be studied directly; and control laws can be designed in a more straightforward way such that unnecessary two-dimensional (2-D) to 3-D estimation can be bypassed.
- 3) One could generalize our results to the case of a camera mounted on an aircraft performing visual servoing. In this case there is no fixed homography between ground curves and the image plane.

Note that ξ and ζ are still functions of y (or Y). They need to be evaluated at a fixed y (or Y). Since the ground curve Γ is analytic, it does not matter at which specific y they are evaluated (as long as the relation between ξ and ζ is well-defined according to Lemma 1).⁵ However, evaluating ξ or ζ at some special y might simplify the formulation of some control tasks.

For example, suppose a mobile robot is to track the given ground curve Γ . When the mobile robot is perfectly tracking the given curve Γ , i.e., the wheel keeps touching the curve, the orthographic projection image $\tilde{\Gamma} = (\gamma_x(y, t), y)^T$ of the curve Γ should satisfy

$$\gamma_x(y, t)|_{y=-d \cos \phi} \equiv 0. \quad (20)$$

Furthermore, the tangent to the curve Γ at $y = -d \cos \phi$ should be in the same direction as the mobile robot. This requires

$$\left. \frac{\partial \gamma_x(y, t)}{\partial y} \right|_{y=-d \cos \phi} \equiv 0. \quad (21)$$

Thus, if ξ is evaluated at $y = -d \cos \phi$, the task of tracking Γ becomes a control problem of steering both ξ_1 and ξ_2 to 0 for the system (13). *For these reasons, from now on, we always evaluate ξ (or ζ) at $y = -d \cos \phi$ unless explicitly stated.*

A. Controllability in the Linear Curvature Curve Case

If the given ground curve Γ is a linear curvature curve, the dynamics of its image is given by (18).

Theorem 1: (Dimension of Controllability Lie Algebra) Consider the system (18)

$$\dot{\xi}^3 = f_1 \omega + f_2 v \quad (22)$$

⁵For analytic curves, there is a one-to-one correspondence between the two sets of coefficients of the Taylor series expanded at two different points.

where the vector fields (f_1, f_2) are

$$f_1 = - \begin{bmatrix} \xi_1 \xi_2 \sin \phi + d \cot \phi + \frac{y}{\sin \phi} \\ \xi_1 \xi_3 \sin \phi + \xi_2^2 \sin \phi + \frac{1}{\sin \phi} \\ \xi_1 \xi_4 \sin \phi + 3 \xi_2 \xi_3 \sin \phi \end{bmatrix}$$

$$f_2 = \begin{bmatrix} \xi_2 \sin \phi \\ \xi_3 \sin \phi \\ \xi_4 \sin \phi \end{bmatrix}$$

and $\xi_4 = (c(a^2 + \xi_2^2)^3/a + 3\xi_2\xi_3^2/a^2 + \xi_2^2)$. If $\phi \neq 0$, and $y = -d \cos \phi$, then the distribution $\Delta_{\mathcal{L}}$ spanned by the Lie algebra $\mathcal{L}(f_1, f_2)$ generated by (f_1, f_2) is of rank 3 when and is of rank 2 when $c = 0$.

Proof: Directly calculate the Lie bracket $[f_1, f_2]$

$$[f_1, f_2] = (-1, 0, 0)^T. \quad (23)$$

The determinant of matrix $(f_1, f_2, [f_1, f_2])$ is

$$\det(f_1, f_2, [f_1, f_2]) = -c(a^2 + \xi_2^2)^3/a^3. \quad (24)$$

Therefore, the distribution $\Delta_{\mathcal{L}}$ spanned by $\mathcal{L}(f_1, f_2)$ is of rank 3 if $c \neq 0$, and of rank 2 if $c = 0$. ■

Since $\Delta_{\mathcal{L}}$ is of full rank at all points, it is involutive as a distribution. Chow's Theorem [14] states that the reachable space of system (18) for ξ^3 is of dimension 3 when $c \neq 0$, and 2 when $c = 0$. This makes sense since, when $c = 0$, i.e., the case of constant curvature curves, there are only two independent parameters, ξ_1 and ξ_2 , needed to describe the image curves, the reachable space of such system can be at most dimension 2.

B. General Case

We now consider the general case of an *arbitrary* ground mobile robot tracking an arbitrary analytic ground (planar) curve. Since the dynamics of the mobile robot are now assumed to be general, one can no longer get an explicit expression of the dynamics of the system ξ as we did in the unicycle case. However, the set of all possible motions of any ground-based mobile robot, regardless of the dynamics, turns out to be in the same space: i.e., the group of planar rigid body motions $SE(2)$. Then locally there is a map from this group to the reachable space of ξ (or ζ). For a detailed discussion, please refer to the technical report [18]. In particular, we have:

Theorem 2: (Dimension of Controllability Lie Algebra for Arbitrary Planar Mobile Robot)

Consider an arbitrary ground-based mobile robot and an arbitrary planar analytic curve $\Gamma = (\gamma_x(y), y, \gamma_z(y))^T$ with γ_z given by (3). ξ is defined as the vector of the coefficients of the Taylor series of $\gamma_x(y)$ expanded at $y = -d \cos \phi$.⁶ Then (i) the (locally) reachable space of ξ under the motion of the mobile robot has at most 3 dimensions; (ii) if under the motion of the mobile robot, ξ (and ζ) is also a dynamic system, the rank of the distribution spanned by the Lie algebra generated by the vector fields associated to such a system is at most 3.

⁶This definition of ξ turns out to be exactly the same as we defined in (5).

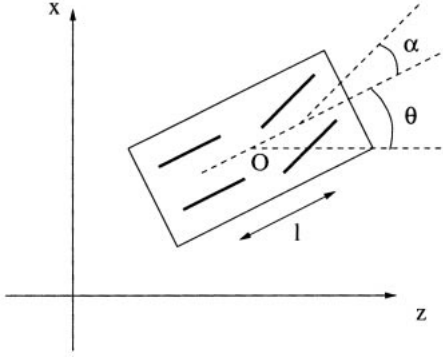


Fig. 5. Front wheel drive car with a steering angle α and a camera mounted above the center O.

This theorem highlights the importance of Theorem 1 from two aspects: the controllable space is of dimension at most 3 for controlling the shape of the image of an arbitrary curve, which means linear curvature curves already capture all the features $(\xi_1, \xi_2, \xi_3)^T$ that may be totally controlled; on the other hand, any other nonholonomic mobile robot cannot do essentially “better” in controlling the shape of the image curve than the unicycle. Combining this theorem with the previous results about the unicycle and the linear curvature curves, we have the following corollaries:

Corollary 1: Consider a linear curvature curve (i.e., $k'(s) = c \neq 0$) and an arbitrary maximally nonholonomic ground-based mobile robot, the reachable space of ξ^3 (and ζ^3) under the motion of the robot is (locally) of dimension 3. Furthermore, if under the motion of this mobile robot, ξ^3 (and ζ^3) is itself a dynamic system, then the rank of the distribution spanned by the Lie algebra generated by the vector fields associated to such a system is exactly 3.

This corollary is true because, for a special nonholonomic mobile robot: the unicycle, according to Theorem 1, the local reachable space has exactly dimension 3 in the case of linear curvature curves. For any two maximally nonholonomic ground-based mobile robots, their motion spaces are the same as $SE(2)$. Thus they have the same ability to control the shape of the image curve.

In the case of the unicycle, as already derived in Section II-B2, ξ is a dynamic system given by (13), therefore we can state the following corollary:

Corollary 2: The rank of the distribution spanned by the Lie algebra generated by the vector fields associated with the system (13) is at most 3. In the case of linear curvature curves, the rank is exactly 3 (as previously stated in Theorem 1).

In the case of constant curvature curves, there are only two independent parameters ξ_1 and ξ_2 needed to determine the image curve. Obviously, all the above corollaries still hold by changing rank 3 to rank 2.

C. Front Wheel Drive Car

In this section, we show how to apply the study of unicycle model to the kinematic model of a front wheel drive car as shown in Fig. 5.

The kinematics of the front wheel drive car (relative to the spatial frame) is given by

$$\begin{aligned}\dot{x} &= \sin \theta u_1 \\ \dot{z} &= \cos \theta u_1 \\ \dot{\theta} &= l^{-1} \tan \alpha u_1 \\ \dot{\alpha} &= u_2\end{aligned}\quad (25)$$

where u_1 is the forward velocity of the rear wheels of the car and u_2 is the velocity of the steering rate angle.

The dynamic model of the front wheel drive car, the so called “bicycle model” [19] has the same inputs and the same kinematics as this kinematic model of the car. In the dynamic setting the lateral and longitudinal dynamics are typically decoupled in order to obtain two simpler models. The lateral dynamics model used for the design of the steering control laws captures the system dynamics in terms of lateral velocity (or alternatively slip angle) and yaw rate. The control laws derived using this kinematic model are applicable to the highway driving scenarios providing that the 3-D effects of the road curvature are negligible and the variations in the pitch angle can be compensated for. Under normal operating conditions and lower speeds the dynamical effects are not so dominant. Comparing (25) to the kinematics of the unicycle, we have

$$\omega = l^{-1} \tan \alpha u_1, \quad v = u_1. \quad (26)$$

If we rewrite the system (13) as

$$\dot{\xi} = f_1 \omega + f_2 v \quad (27)$$

the dynamics of the image of a ground curve under the motion of the front wheel drive car is given by

$$\begin{bmatrix} \dot{\alpha} \\ \dot{\xi} \end{bmatrix} = \begin{bmatrix} 0 \\ l^{-1} \tan \alpha f_1 + f_2 \end{bmatrix} u_1 + \begin{bmatrix} 1 \\ 0 \end{bmatrix} u_2 \quad (28)$$

or simply as

$$\begin{bmatrix} \dot{\alpha} \\ \dot{\xi} \end{bmatrix} = \tilde{f}_1 u_1 + \tilde{f}_2 u_2$$

for obvious \tilde{f}_1, \tilde{f}_2 . Calculating the controllability Lie algebra for this system, we get

$$\begin{aligned}\tilde{f}_2 &= \begin{bmatrix} 1 \\ 0 \end{bmatrix}, \quad \tilde{f}_1 = \begin{bmatrix} 0 \\ l^{-1} \tan \alpha f_1 + f_2 \end{bmatrix} \\ [\tilde{f}_1, \tilde{f}_2] &= \begin{bmatrix} 0 \\ -l^{-1} \sec^2 \alpha f_1 \end{bmatrix} \\ [\tilde{f}_1, [\tilde{f}_1, \tilde{f}_2]] &= \begin{bmatrix} 0 \\ l^{-1} \sec^2 \alpha [f_1, f_2] \end{bmatrix}.\end{aligned}$$

Clearly, as long as $\sec^2 \alpha \neq 0$, i.e., α is away from $\pm\pi/2$, we have

$$\text{rank}(\tilde{f}_1, [\tilde{f}_2, \tilde{f}_1], [\tilde{f}_1, [\tilde{f}_2, \tilde{f}_1]]) = \text{rank}(f_1, f_2, [f_1, f_2]). \quad (29)$$

Thus, the controllability for the front wheel drive car is the same as the unicycle. As a corollary to Theorem 1, we have

Corollary 3: For a linear curvature curve, the rank of the distribution spanned by the Lie algebra generated by the vector fields associated with the system (28) is exactly 4. For constant curvature curves, i.e., straight lines or circles, the rank is exactly 3.

Combining this result with Theorem 2, under the motion of the front wheel drive car, the shape of a image curve is controllable only up to its linear curvature terms, as is the unicycle case.

IV. CONTROL DESIGN IN THE IMAGE PLANE

In this section, we study the design of control laws for controlling the shape of the image curve in the image plane so as to facilitate successful navigation of the ground-based mobile robot.

A. Controlling the Shape of Image Curves

According to the controllability results presented in the previous section, one can only control up to three parameters $(\xi_1, \xi_2, \xi_3)^T$ of the image of a given ground curve. This means the shape of the image curve can only be controlled up to the linear curvature features of a given curve. In this section, we study how to obtain control laws for controlling the image of a linear curvature curve, as well as propose how to control the image of a general curve.

1) *Unicycle:* For a unicycle mobile robot, the dynamics of the image of a linear curvature ground curve is given by system (18). According to Theorem 1, this two-input 3-D system is controllable (i.e., has one degree of nonholonomy) for $c \neq 0$. Thus, using the algorithm given in Murray and Sastry [14], [15], system (18) can be transformed to the canonical *chained-form*. The resulting change of coordinates is

$$\begin{aligned} x_1 &= \xi_2 \\ x_2 &= -\frac{a^3 \xi_3}{c(a^2 + \xi_2^2)^3} \\ x_3 &= \left(\xi_1 - \frac{a \xi_2 \xi_3}{c(a^2 + \xi_2^2)^2} \right) \\ \omega &= \frac{-ca(a^2 + \xi_2^2)^3 + 3a^2 \xi_2 \xi_3^2}{c(a^2 + \xi_2^2)^4} u_1 - \frac{\xi_3}{a} u_2 \\ v &= \frac{-ca(a^2 + \xi_2^2)^3 + 3a^2 \xi_2 \xi_3(a^2 + \xi_2^2 + \xi_3)}{c(a^2 + \xi_2^2)^4} u_1 \\ &\quad - \frac{a^2 + \xi_2^2 + \xi_3}{a} u_2 \end{aligned}$$

where $a = (\sin \phi)^{-1}$. Then, the transformed system has the chained-form

$$\begin{aligned} \dot{x}_1 &= u_1 \\ \dot{x}_2 &= u_2 \\ \dot{x}_3 &= x_2 u_1. \end{aligned} \quad (30)$$

For the chained-form system (30), using *piecewise smooth sinusoidal inputs* [15], one can arbitrarily steer the system from one point to another in \mathbb{R}^3 . More robust closed loop control schemes based on time varying feedback techniques can also

be found in [22]. In principle, one can therefore control the shape of the image of a linear curvature curve.

Note that when $c = 0$, i.e., the curve is of constant curvature, the above transformation is not well-defined. This is because the system ξ now only has two independent states ξ_1 and ξ_2 . It is much easier to steer such a two-input two-state system than the above chained-form system.

Remark 2: Using Lemma 1, the dynamic system ζ^3 of the perspective projection image of a linear curvature curve can be also transformed to chained-form.

2) *Front Wheel Drive Car:* In this section we show that the image curve dynamical system (28) for the front wheel drive car model is also convertible to chained-form. According to Tilbury [23], the necessary and sufficient conditions for a system to be convertible to the chained-form are given by the following theorem:

Theorem 3: (Murray [24])

Consider a n -dimensional system with two inputs u_1, u_2

$$\dot{x} = g_1 u_1 + g_2 u_2, \quad x \in \mathbb{R}^n. \quad (31)$$

Let the distribution $\Delta = \text{span}\{g_1, g_2\}$ and define two nested sets of distributions

$$\begin{aligned} E_0 &= \Delta, & F_0 &= \Delta, \\ E_1 &= E_0 + [E_0, E_0], & F_1 &= F_0 + [F_0, F_0] \\ E_2 &= E_1 + [E_1, E_1], & F_2 &= F_1 + [F_1, F_1] \\ &\vdots & &\vdots \\ E_{i+1} &= E_i + [E_i, E_i], & F_{i+1} &= F_i + [F_i, F_0]. \end{aligned}$$

The system is convertible to chained-form if and only if

$$\dim(E_i) = \dim(F_i) = i + 2, \quad i = 0, \dots, n - 2.$$

Then we can directly check the two sets of distributions for the dynamical system (28) of the image curve for the front wheel drive car

$$\begin{bmatrix} \dot{\alpha} \\ \dot{\xi} \end{bmatrix} = \tilde{f}_1 u_1 + \tilde{f}_2 u_2. \quad (32)$$

$$\begin{aligned} E_0 &= F_0 = \text{span}\{\tilde{f}_1, \tilde{f}_2\} \\ E_1 &= F_1 = \text{span}\{\tilde{f}_1, \tilde{f}_2, [\tilde{f}_1, \tilde{f}_2]\}. \end{aligned}$$

Clearly, $[\tilde{f}_1, [\tilde{f}_1, \tilde{f}_2]] \in [F_1, F_0] \subset F_2$. For a linear curvature curve, (32) is a four-dimensional (4-D) system. According to Corollary (3), $\dim(F_2) = \dim(F_1 + [F_1, F_0]) = 4$. Since $F_2 \subset E_2$, we have $\dim(E_2) = \dim(F_2) = 4$. Thus, according to Theorem 3, the system (28) is convertible to chained-form. The coordinate transformation may be obtained using the method given by Tilbury *et al.* in [23].

Everything we discussed in the previous section for the unicycle also applies to the kinematic front wheel drive car model. In the rest of the paper, only the unicycle case will be studied in detail but it is easy to generalize all the results to the car model as well.

B. Tracking Ground Curves

In this section, we formulate the problem of mobile robot tracking a ground curve as a problem of controlling the shape of its image with the dynamics described by (13). We design a *state feedback* control law for this system such that the mobile robot (unicycle) asymptotically tracks the given curve.

First, let us study the *necessary and sufficient conditions* for perfect tracking of a given curve. As already explained at the beginning of Section III, when the mobile robot is perfectly tracking the given curve

$$\xi_1 = \gamma_x(y, t)|_{y=-d \cos \phi} \equiv 0 \quad (33)$$

$$\xi_2 = \frac{\partial \gamma_x(y, t)}{\partial y} \Big|_{y=-d \cos \phi} \equiv 0. \quad (34)$$

From (18) when $\xi_1 = \xi_2 \equiv 0$, we have $\dot{\xi}_2 = -\xi_3 v \sin \phi + \omega / \sin \phi \equiv 0$. This gives the *perfect tracking angular velocity* $\omega = \xi_3 \sin^2 \phi v$.

It is already known that system (13) is a nonholonomic system. According to Brockett [20], there do not exist smooth state feedback control laws which asymptotically stabilize a *point* of a nonholonomic system. However, it is still possible that smooth control laws exist for the mobile robot to asymptotically track a given curve, i.e., to stabilize the system ξ around the subset $M = \{\xi \in \mathbb{R}^\infty: \xi_1 = \xi_2 = 0\}$. We first give a control law which stabilizes the system around the set M in the Lyapunov sense. The idea is based on a “partial” Lyapunov function.

Theorem 4: (Stabilizing Control Laws)

Consider closing the loop of system ξ (13) with control (ω, v) given by

$$\begin{aligned} \omega &= \xi_3 \sin^2 \phi v_0 + \sin^2 \phi \xi_1 v_0 + K_\omega \xi_2 \\ v &= v_0 + \sin^2 \phi \xi_1 (\xi_1 + \xi_3) v_0 - K_v \xi_2 \operatorname{sign}(\xi_1 + \xi_3) \end{aligned} \quad (35)$$

where K_ω, K_v are strictly positive constants. The closed-loop system is stable around the subset

$$M = \{\xi \in \mathbb{R}^\infty: \xi_1 = \xi_2 = 0\} \quad (36)$$

for initial conditions with ξ_1 and ξ_2 small enough. Once on M , the mobile robot has the given linear velocity v_0 and the perfect tracking angular velocity $\omega_0 = \xi_3 \sin^2 \phi v_0$.

Proof: Consider the “partial” Lyapunov function $V = \xi_1^2 + \xi_2^2$. Through direct calculation, we get

$$\begin{aligned} \dot{V} &= -K_\omega / \sin \phi \xi_2^2 - K_\omega \sin \phi \xi_2^4 \\ &\quad - \xi_2^2 \sin \phi [(K_\omega \xi_1 + \xi_2 \sin^2 \phi v_0) \\ &\quad + K_v \operatorname{sign}(\xi_1 + \xi_3)] (\xi_1 + \xi_3). \end{aligned} \quad (37)$$

There exists $\epsilon > 0$ such that, when $|\xi_1| < \epsilon$ and $|\xi_2| < \epsilon$

$$|K_\omega \xi_1 + \xi_2 \sin^2 \phi v_0| < K_v. \quad (38)$$

In the set $W_\epsilon \equiv \{\xi \in \mathbb{R}^\infty: \xi_1^2 + \xi_2^2 < \epsilon^2\}$

$$\dot{V} \leq -K_\omega / \sin \phi \xi_2^2 \leq 0. \quad (39)$$

Thus the system is stable around the set M in the Lyapunov sense. ■

It can be shown that this control law asymptotically stabilizes the system if the overall curvature of the curve ξ_3 is bounded.⁷ It is also shown by simulation that, with appropriately choosing K_v and K_ω , this control law (35) has a very large domain of attraction. However, this control is only locally stable. A global control scheme has been proposed by Hespanha and Morse [25] based on the idea of “partial” feedback linearization.

Proposition 1: (Hespanha and Morse)

For the system ξ (13), set

$$\begin{aligned} v &= v_0 + \xi_1 \omega, \quad v_0 > 0 \\ \omega &= \frac{\sin \phi}{1 + \sin^2 \phi \xi_2^2} (v_0 \sin \phi \xi_3 + a \xi_1 + b \xi_2) \end{aligned} \quad (40)$$

for $a, b > 0$. Then the partial closed loop system of ξ_1, ξ_2 is linearized and given by

$$\begin{aligned} \dot{\xi}_1 &= v_0 \sin \phi \xi_2, \\ \dot{\xi}_2 &= -a \xi_1 - b \xi_2. \end{aligned} \quad (41)$$

This control law guarantees the partial system that we are interested is globally exponentially stable regardless of the boundeness of the curvature. Thus the closed loop mobile robot globally asymptotically tracks an arbitrarily given analytic curve.

In the above, we have assumed that the set point for the linear velocity v_0 is always nonzero. In the case that $v_0 = 0$, both the control laws (35) and (40) are still stable but no longer asymptotically stable. From the partially linearized system (41), ξ_1 remains constant but ξ_2 can still be steered to zero. This makes sense because, without linear velocity, one can only rotate the unicycle and line up its heading with the curve but the distance to the curve remains the same.

1) *Tracking C^1 -Smooth Piecewise Analytic Curves:* Although Theorem 4 only deals with analytic (C^ω) curves, it actually can be generalized to C^1 -smooth piecewise analytic curves⁸.

Corollary 4: Consider an arbitrary C^1 -smooth piecewise analytic (ground) curve. If the maximum curvature $|k|_{\max}$ exists for the whole curve, then, when $K_\omega > 0$ and $K_v \geq 0$ the feedback control law given by (35) guarantees that the mobile robot locally asymptotically tracks the given curve.

Proof: Consider the same Lyapunov function as the one chosen in Theorem 4. Then, \dot{V} is still given by (37). Since $|k|_{\max}$ exists, from (15), $|\xi_3|$ is bounded. Then, according to (37), if $K_\omega > 0$ and $K_v \geq 0$, there exist $\epsilon > 0$, which is independent of ξ_3 , such that when $\xi \in W_\epsilon = \{\xi_1^2 + \xi_2^2 < \epsilon^2\}$

$$\dot{V} \leq -K_\omega / \sin \phi \xi_2^2 \leq 0. \quad (42)$$

The rest of the proof follows that of Theorem 4. ■

⁷The complete proof is quite involved and is thus omitted here.

⁸“ C^1 -smooth” means that the tangent vector along the whole curve is continuous.

It is very important to note that, in the proof of Theorem 4, the choice of ϵ is independent of ξ_3 . For a C^1 -smooth piecewise analytic curve, ξ_1 and ξ_2 are always continuous. Only ξ_3 may not change continuously. But the proof shows that the \dot{V} does not depend on ξ_3 when ξ_1 and ξ_2 are small enough. Therefore the (C^1 -smooth) switching between different analytic pieces of the curve does not affect the convergence of the system. In Corollary 4, since ξ_3 is bounded, K_v can then be set to 0 and the inequality (39) for \dot{V} still holds locally. In the case of $K_v = 0$, the control (35) becomes a smooth one. It is also clear for the feedback linearization control law (40) that the exponential convergence is preserved through C^1 smooth switching between curves.

Remark 3: Using Lemma 1, the control laws (35) or (40) can be converted to a stabilizing tracking control law for ζ of the perspective projection image.

2) *Tracking Arbitrary Curves:* Corollary 4 suggests that, for tracking an arbitrary continuous (C^0 -smooth) ground curve (not necessarily analytic), one may approximate it by a C^1 -smooth piecewise analytic curve, a *virtual curve*, and then track this approximating virtual curve by using the tracking control law. However, since the virtual curve cannot be “seen” in the image, how could one get the estimates of ξ for the “image” of the virtual curve so as to get the feedback controls v and ω subsequently? It turns out that, the virtual ξ is exactly the solution of the differential equation of the closed-loop system (13) with v and w given by the tracking control law. The initial conditions for solving such differential equation can be obtained when designing the virtual curve.

Now, the control becomes an open-loop scheme, and in order to track this virtual curve, one has to solve the differential equation (13) in advance and then get the desired controls v and ω . It is computationally expensive to approximate a given curve by an arbitrary analytic curve in which case, in principle, we have to solve the infinite-dimensional differential equation (13).

However, as argued in Section II-B2, a special class of analytic curves, the linear curvature curves, can reduce the infinite-dimensional system (13) to a 3-D system (18), and the three states ξ^3 of the system (18) also have captured all the controllable features of the system ξ , according to Theorem 2. Therefore, it is much more computationally economical to approximate the given curve by a C^1 -smooth piecewise linear curvature curve and then solve the 3-D differential equation (18) to get the appropriate controls v and ω .

Few applications do require tracking of arbitrary (analytic) curves. The target curves usually can be modeled as piecewise linear curvature curves. For instance, in the case of vehicle control, in the United States, most highways are designed to be of piecewise constant curvature, and in Europe, as clothoids. Therefore, piecewise linear curvature curves are simple as well as good models for most tracking tasks.

Strictly speaking, when approximating a given curve by a piecewise polynomial curve, for example by using splines [12], in order to get the estimate of ξ for the evolution of the approximating virtual curve, one has to solve the infinite-dimensional differential equation (13). What the “polynomial” property really simplifies is just the initial conditions of the

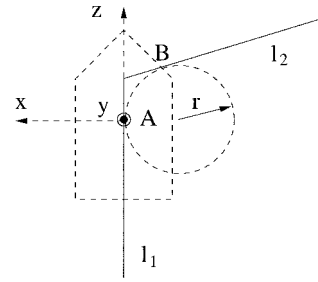


Fig. 6. Using arcs to connect curves which are piecewise straight lines.

differential equation but not the dimension of the problem, as already argued in Section II-B3.

Example: Mobile Robot Tracking Corridors: Consider a simple example: the mobile robot is supposed to track a piecewise linear curve consisting of intersection of l_1 and l_2 (as a reasonable model for corridors inside a building), as shown in Fig. 6. A natural and simple way to smoothly connect them together is to use a piece of arc AB which is tangential to both of the straight lines (at points A and B respectively). From point A , the mobile robot switches to track the virtual curve, arc AB until it smoothly steers into the next piece, i.e., the line l_2 . The $\xi^3(t)$ for tracking this virtual arc AB is then given by the solution of the closed-loop system of (18) with $c = k'(s) \equiv 0$ and the initial conditions at point A : $\xi^3(0) = (0, 0, -a^2/r)^T$.

Since the approximating virtual curve is to be as close to the original curve as possible, the radius r of the arc AB should be as small as possible. But, in real applications, the radius r is limited by the maximal curvature that the mobile robot can track ($r = 1/|k|$). Thus, one needs to consider this extra constraint when designing the virtual curves. The following result tells us a way to decide the maximal curvature $|k|_{\max}$ that the mobile robot can track:

Fact 1: Consider the unicycle mobile robot. If its linear velocity v and angular velocity ω satisfy $|v| \geq c_1$ and $\omega^2 + v^2 \leq c_2^2$, then the maximal curvature that it can track is

$$|k| \leq \sqrt{\left(\frac{c_2}{c_1}\right)^2 - 1}. \quad (43)$$

Consider now that the image curve obtained is not even continuous, i.e., the robot “sees” several pieces of the image of the real curve that it is supposed to track. Basically, there are two different approaches that one might take in order to track such a curve: first, one may use some estimation schemes and based on the estimated features of the real curve to apply the feedback control law (as studied by Frezza and Picci [12]); second, one may just smoothly connect these pieces of the image curve by straight lines, arcs or linear curvature curves and then apply the virtual tracking scheme as given above to track the approximating virtual curves.

C. Simulation Results of Tracking Ground Curves

In this section, we show simulation results of the mobile robot tracking some specific ground curves using the control schemes designed in previous sections. We assume that all the

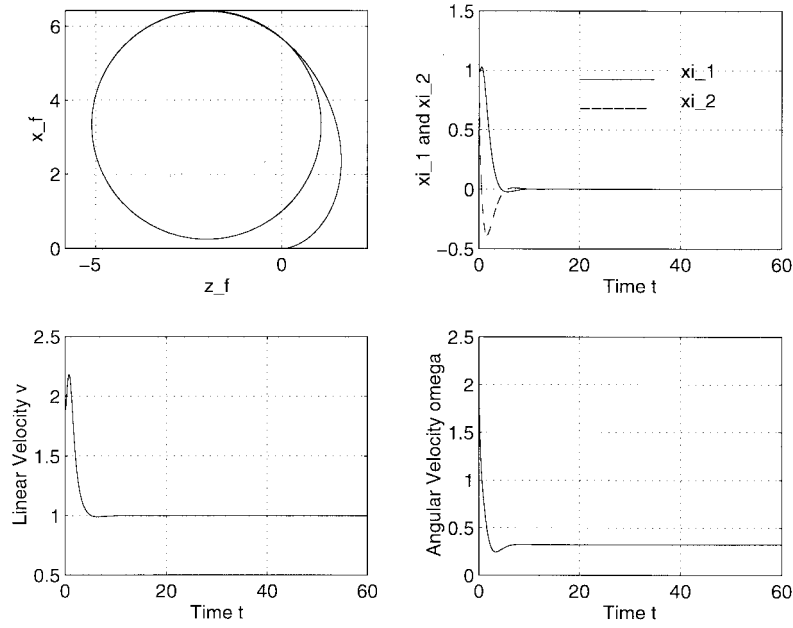


Fig. 7. Simulation results for tracking a circle. Subplot 1: the trajectory of the mobile robot in the reference coordinate frame; subplot 2: the image curve parameters ξ_1 and ξ_2 ; subplot 3 and 4: the control inputs v and ω .

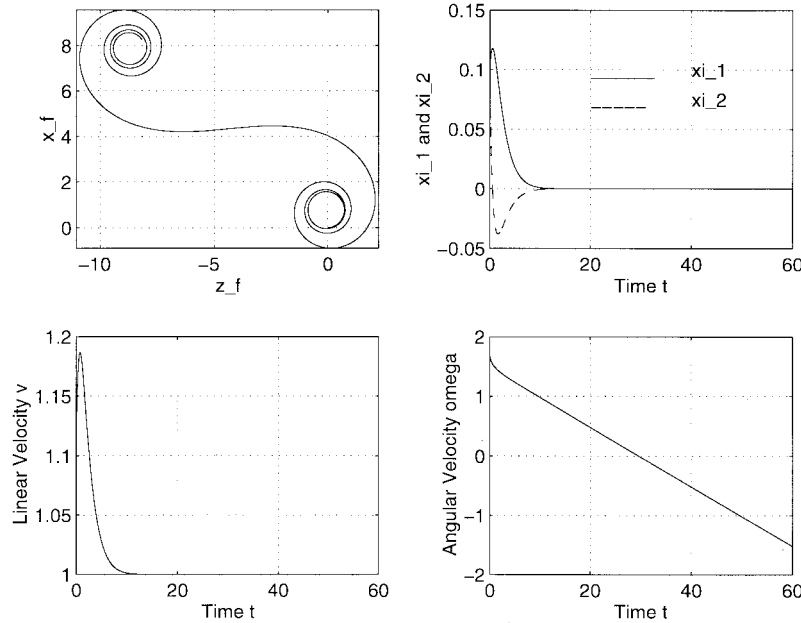


Fig. 8. Simulation results for tracking a linear curvature curve ($c = k'(s) = -0.05$). Subplot 1: the trajectory of the mobile robot in the reference coordinate frame; subplot 2: the image curve parameters ξ_1 and ξ_2 ; subplot 3 and 4: the control inputs v and ω .

image features ξ are already available. In the next section, we discuss how to actually estimate ξ from the real images corrupted by noise. For all the following simulations, we choose the camera tilt angle $\phi = \pi/3$, and the control parameters $K_\omega = 1, K_v = 0.5$, and $v_0 = 1$. The reference coordinate frame F_f is chosen such that the initial position of the mobile robot is $z_{f0} = 0, x_{f0} = 0$ and $\theta_0 = 0$.

1) *Tracking a Circle*: A circle is a constant curvature curve, i.e., $c = k'(s) \equiv 0$. For the simulation results shown in Fig. 7, the initial position of the nominal circle given in the image plane is $\xi_{10} = 1, \xi_{20} = 1$, and $\xi_{30} = 1$.

2) *Tracking a Linear Curvature Curve*: For the simulation results given in Fig. 8, the nominal trajectory is chosen to be a linear curvature curve with the constant curvature varying rate $c = k'(s) \equiv -0.05$. Its initial position given in the image plane is $\xi_{10} = 0.1, \xi_{20} = 0.1$, and $\xi_{30} = 2$.

3) *Tracking Piecewise Straight-Line Curves*: Consider now the example discussed in Section IV-B2: the mobile robot is to track a piecewise linear curve consisting of intersection of l_1 and l_2 as shown in Fig. 9. We compare the simulation results of two schemes:

- 1) using only the feedback tracking control law;

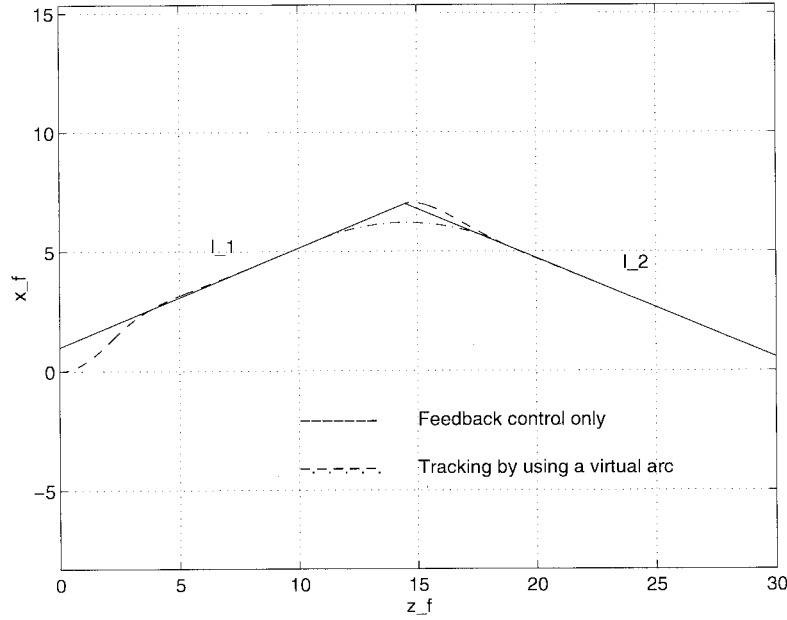


Fig. 9. Comparison between two schemes for tracking a piecewise straight-line curve.

- 2) using a pre-designed approximating virtual curve (an arc in this case) around the intersection point.

From Fig. 9, it is obvious that, by using the pre-designed virtual curve, the over-shoot can be avoided. But the computation is more intensive: one needs to design the virtual curve and calculate the desired control inputs for tracking it.

V. OBSERVABILITY ISSUES AND ESTIMATION OF IMAGE QUANTITIES

As we have discussed in Section II-B1, ξ are the features of the orthographic projection image $\hat{\Gamma}$ of the ground curve Γ , and are not yet the real image (which, by convention, means the perspective projection image Λ) quantities ζ . However, ξ and ζ are algebraically related by Lemma 1. In principle, one can obtain ξ from the directly-measurable ζ .

In order to apply the tracking control laws given before, one need to know the values of ξ_1, ξ_2 , and ξ_3 , i.e., ζ_1, ζ_2 , and ζ_3 . Suppose, at each instant t , the camera provides N measurements of the image curve Λ

$$\{(\lambda_X(Y_k, t), Y_k)\}, \quad k = 1, \dots, N \quad (44)$$

where $\{Y_1, Y_2, \dots, Y_N\}$ are fixed distances from the origin. If the distances between Y_k are small enough, one can estimate the values of $\zeta_1(Y_k), \zeta_2(Y_k)$, and $\zeta_3(Y_k)$ simply by

$$\begin{aligned} \hat{\zeta}_1(Y_k) &= \lambda_X(Y_k, t) \\ \hat{\zeta}_2(Y_k) &= \frac{\hat{\zeta}_1(Y_{k+1}) - \hat{\zeta}_1(Y_k)}{Y_{k+1} - Y_k} \\ \hat{\zeta}_3(Y_k) &= \frac{\hat{\zeta}_2(Y_{k+1}) - \hat{\zeta}_2(Y_k)}{(Y_{k+1} - Y_k)} \end{aligned} \quad (45)$$

for $k = 1, \dots, N-2$. However, in practice, the measurements $\{(\lambda_X(Y_k, t), Y_k)\}$ are noisy and the estimates (45) for ζ^3 become very inaccurate, especially for the higher order terms

ζ_2 and ζ_3 . It is thus appealing to estimate ζ^3 or ξ^3 by only using the measurements $\{(\lambda_X(Y_k, t), Y_k)\}$ but not their differences.

A. Sensor Models and Observability Issues

The curve dynamics are already given by (13). If we only use the measurement $\zeta_1 = \lambda_X(Y, t)$ as the output of the vision sensor, then we have the following sensor model:

$$\begin{aligned} \dot{\xi} &= f_1 \omega + f_2 v \\ h(\xi) &= \zeta_1 = \frac{\sin \phi}{d + y \cos \phi} \xi_1 \end{aligned} \quad (46)$$

where f_1, f_2 are the same as in (13) and $h(\xi)$ is the measurable output of the system.

Theorem 5: (Observability of the Camera System)

Consider the system given by (46). If $\phi \neq 0$, then the annihilator Q of the smallest codistribution Ω invariant under f_1, f_2 and which contains $dh(\xi)$ is empty.

Proof: Through direct calculations, the k th order Lie derivative of the covector field $dh(\xi)$ along the vector field f_2 is

$$L_{f_2}^k dh(\xi) = \frac{\sin^{k+1} \phi}{d + y \cos \phi} d\xi_{k+1}, \quad k \in \mathbb{N}. \quad (47)$$

Thus, Ω contains all $d\xi_i$ and therefore Q is an empty distribution. ■

According to the Theorem 1.9.8 in Isidori [26], Theorem 5 guarantees that the system (46) is observable. In other words, the (locally) *maximal output zeroing manifold* of the system (46) does not exist, according to the Proposition 10.16 in Sastry [27]. Since this system is observable, ideally, one then can estimate the $\hat{\xi}$ from the output $h(\xi)$. However, the observer construction may be difficult.

1) *Linear Curvature Curves*: The sensor model (46) is an infinite-dimensional system. In order to build an applicable estimator for ξ^3 (so as to apply the tracking control laws), one has to assume some regularity on the given curve Γ so that the sensor model becomes a finite-dimensional system. In other words, one has to approximate Γ by simpler curve models which have finite-dimensional dynamics.

In Frezza and Picci [12], the models chosen are *third-order B-splines*. However, as we have pointed out in Section II-B3, the polynomial form is not an intrinsic property of a curve and it cannot be preserved under the motion of the mobile robot. Furthermore, simple curves like a circle cannot be expressed by third-order B-splines. We thus propose to use (piecewise) linear curvature curves as the models. The reasons for this are obvious from the discussions in previous sections: the dynamics of a linear curvature curve is a 3-D system (18); such a system has very nice control properties; and piecewise linear curvature curves are also natural models for highways. However, a most important reason for using linear curvature curves is that, according to Theorem 4, one actually only needs the estimation of three image quantities, i.e., ξ_1, ξ_2 , and ξ_3 to be able to track any analytic curve. All the “higher order terms” $\xi_i, i \geq 4$ are not necessary.

For a linear curvature curve, since we do not have a priori knowledge about the constant curvature varying rate $c = k'(s)$, we also need to estimate it. Let $\eta = c$ and we have the following sensor model for linear curvature curves:

$$\begin{aligned} \begin{bmatrix} \dot{\xi}^3 \\ \dot{\eta} \end{bmatrix} &= \begin{bmatrix} f_1^3 \\ 0 \end{bmatrix} \omega + \begin{bmatrix} f_2^3 \\ 0 \end{bmatrix} v \\ h(\xi^3, \eta) &= \zeta_1 = \frac{\sin \phi}{d + y \cos \phi} \xi_1 \end{aligned} \quad (48)$$

where f_1^3, f_2^3 are as in (18) and $h(\xi^3, \eta)$ is the measurable output.

Theorem 6: (Observability of the Simplified Sensor Model)

Consider the system (48). Let

$$f_1 = \begin{bmatrix} f_1^3 \\ 0 \end{bmatrix}, \quad f_2 = \begin{bmatrix} f_2^3 \\ 0 \end{bmatrix}. \quad (49)$$

If $\phi \neq 0$, then the smallest codistribution Ω invariant under f_1, f_2 and which contains $dh(\xi^3, \eta)$ is of constant rank 4.

Proof: Through direct calculations, we have

$$L_{f_2}^k dh(\xi^3, \eta) = \frac{\sin^{k+1} \phi}{d + y \cos \phi} d\xi_{k+1}, \quad k = 0, 1, 2 \quad (50)$$

$$L_{f_2}^3 dh(\xi^3, \eta) = \frac{(a^2 + \xi_2^2) \sin^5 \phi}{d + y \cos \phi} d\eta. \quad (51)$$

Thus, Ω contains all $d\xi_1, d\xi_2, d\xi_3$, and $d\eta$ and it has constant rank 4. ■

Therefore, the system (48) is observable according to the Theorem 1.9.8 in Isidori [26] or the Proposition 10.16 in Sastry [27].

B. Estimation of Image Quantities by Extended Kalman Filter

The sensor model (48) is a nonlinear observable system. The *extended Kalman filter* (EKF) is a widely used scheme

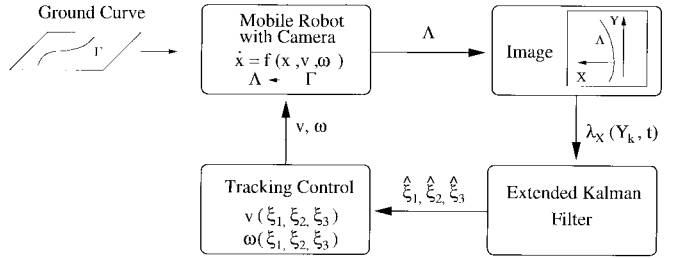


Fig. 10. Closed-loop vision-guided navigation system for a ground-based mobile robot.

to estimate the states of such systems. In the computer vision community, estimation schemes based on Kalman filter have been commonly used for dynamical estimation of motion [3], [28] or road curvature [6], [7]. Here, we use the EKF algorithm to estimate on-line the $\hat{\xi}_1, \hat{\xi}_2, \hat{\xi}_3$, and $\hat{\eta}$. Alternatives to the EKF, which are based on nonlinear filtering, are quite complicated and are rarely used.

In order to make the EKF converge faster, we need to use more than one measurement [in the sensor models (46) and (48)]. From the N measurements

$$\{(\lambda_X(Y_k, t), Y_k)\}, \quad k = 1, \dots, N \quad (52)$$

we have N outputs

$$h_k(\xi) = \zeta_1(Y_k) = \frac{\sin \phi}{d + y_k \cos \phi} \xi_1(y_k) \quad k = 1, \dots, N \quad (53)$$

where Y_k and y_k are related by (4) $Y_k = \frac{y_k \sin \phi}{d + y_k \cos \phi}$.

For linear curvature curves, all the measurements $\xi_1(y_k)$ are functions of only ξ^3 and the linear curvature η since all the Taylor series expansion coefficients $\xi_i, i \in \mathbb{N}$ are functions of only ξ^3 and η according to Lemma 2. Let

$$h(\xi^3, \eta, y) = \sum_{i=1}^{\infty} \frac{\xi_i}{(i-1)!} (y + d \cos \phi)^{i-1}. \quad (54)$$

$\xi_1(y_k)$ are then given by $\xi_1(y_k) = h(\xi^3, \eta, y_k)$. The sensor model (48) can be modified as

$$\begin{aligned} \begin{bmatrix} \dot{\xi}^3 \\ \dot{\eta} \end{bmatrix} &= \begin{bmatrix} f_1^3 \\ 0 \end{bmatrix} \omega + \begin{bmatrix} f_2^3 \\ 0 \end{bmatrix} v \\ h_k(\xi^3, \eta) &= \zeta_1(Y_k) = \frac{\sin \phi}{d + y_k \cos \phi} h(\xi^3, \eta, y_k) \end{aligned} \quad (55)$$

where $k = 1, \dots, N$, and h_k are the measurable outputs.

In order to track the variations in the rate of change of the curvature of a curve, we choose $\dot{\eta} = \mu_\eta$, where μ_η is white noise of appropriate variance.⁹

The output measurements are inevitably noisy, and the actual ones are given by

$$h_k(\xi^3, \eta) = \zeta_1(Y_k) = \frac{\sin \phi}{d + y_k \cos \phi} h(\xi^3, \eta, y_k) + \mu_{h_k} \quad (56)$$

where $k = 1, \dots, N$ and μ_{h_k} are appropriate noise models for the N outputs. Strictly speaking, μ_{h_k} are color noise processes

⁹One may also model η as a second order random walk.

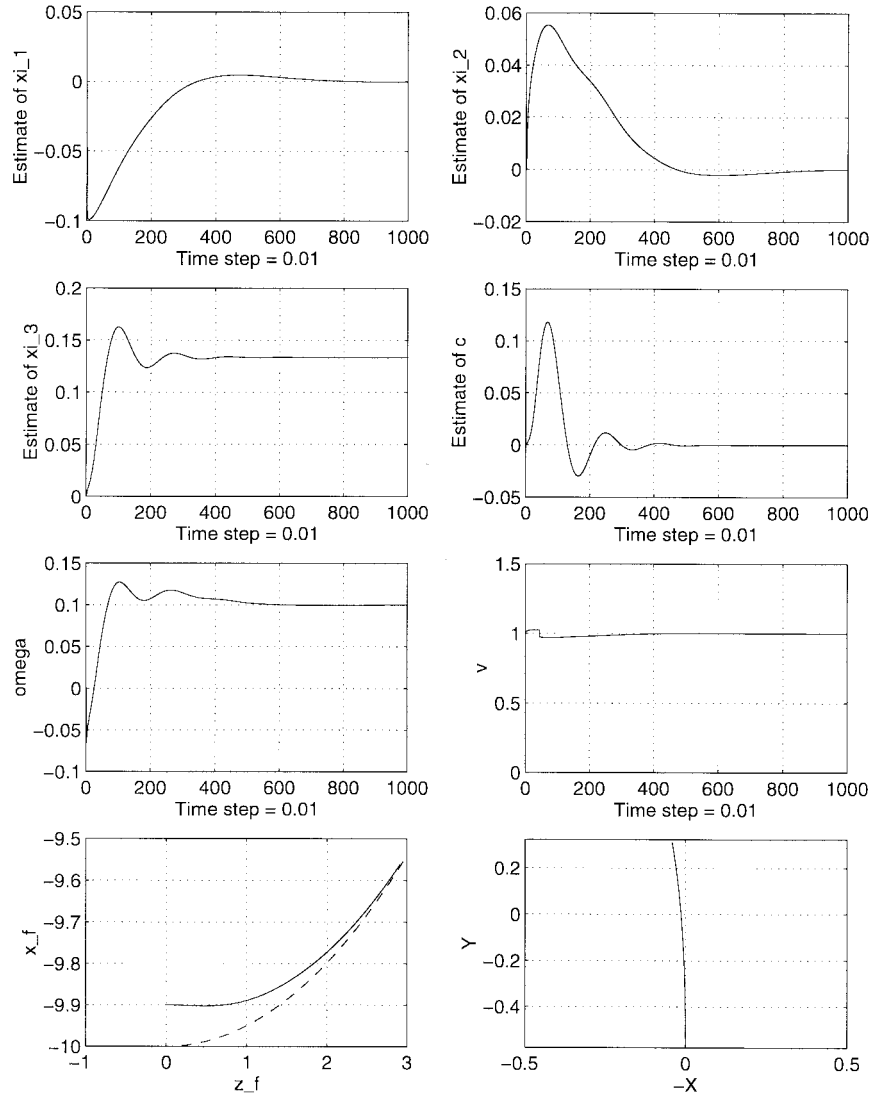


Fig. 11. Simulation results for the closed-loop vision-guided navigation system for the case when the ground curve is a circle: In subplot 7, the solid curve is the actual mobile robot trajectory (in the space frame F_f) and the dashed one is the nominal circle; subplot 8 is the image of the circle viewed from the camera at the last simulation step, when the mobile robot is perfectly aligned with the circle.

since image quantization errors¹⁰ are main sources for μ_{h_k} which generically produce color noise. The explicit forms for the output h_k are given by the Taylor series expansion (54). Truncating the higher order terms of the expansion can be regarded as another color noise source for the output noise μ_{h_k} . However, in order to approximately estimate the states ξ^3 and η , we may simplify μ_{h_k} to white noise processes and then actually build an extended Kalman filter (Jazwinski [29], Mendel [30]) to get the estimates $\hat{\xi}^3$ and $\hat{\eta}$ for the states of the nonlinear stochastic model

$$\begin{aligned} \begin{bmatrix} \dot{\xi}^3 \\ \dot{\eta} \end{bmatrix} &= \begin{bmatrix} f_1^3 \\ 0 \end{bmatrix} \omega + \begin{bmatrix} f_2^3 \\ 0 \end{bmatrix} v + \begin{bmatrix} 0 \\ 1 \end{bmatrix} \mu_\eta, \\ h_k(\xi^3, \eta) &= \zeta_1(Y_k) = \frac{\sin \phi}{d + y_k \cos \phi} h(\xi^3, \eta, y_k) + \mu_{h_k} \end{aligned} \quad (57)$$

where $k = 1, \dots, N$ and μ_η and μ_{h_k} are white noises with appropriate variances. For a detailed implementation of this

¹⁰Including the errors introduced by the image-processing algorithms used to process the original images.

extended Kalman filter, one may refer to the technical report [18].

VI. SIMULATION AND ANIMATION OF THE VISION GUIDED NAVIGATION SYSTEM

In the previous sections, we have developed control and estimation schemes for mobile robot navigation (tracking given curves) using vision sensors. The image parameters needed for the tracking control schemes can be efficiently estimated from direct, probably noisy, image measurements. Combining the control and estimation schemes together, we thus obtain a complete *closed-loop vision-guided navigation system* which is outlined in Fig. 10.

In order to know how this system works, we simulate it by using synthetic images of the ground curve. A *synthetic image* of a ground curve $\Gamma = (\gamma_x(y, t), y, \gamma_z(y, t))^T$ is a set of image points

$$I = \{(\lambda_X(Y_i, t), Y_i)^T = \pi \circ (\gamma_x(y_i, t), y_i, \gamma_z(y_i, t))^T\}_{i=1}^M$$

where π denotes the perspective projection map and the number of image points M maybe different for different time t . The output measurements from this synthetic image I are taken at N pre-fixed distances: Y_1, \dots, Y_N . *Linear interpolation* is used to obtain an approximate value of $\lambda_X(Y_k, t)$ if there is no point in I whose Y coordinate is Y_k .

Simulation results show that the control and the estimation schemes work well with each other in the closed-loop system. For illustration, Fig. 11 presents the simulation results for the simple case when Γ is a circle.

VII. DISCUSSION AND FUTURE WORK

In order to use the vision sensors inside the control servo loop, one first needs to study the dynamics of the features in the image. The dynamics of certain simple geometric primitives, like points, planes and circles, have been studied and exploited by Espiau [11] Pissard-Gibollet and Rives [11] *et al.*. In this paper, we show that, for ground-based mobile robot, it is possible to study the dynamics of the image of a more general class of objects: analytic curves. Based on the understanding of image curve dynamics, we design control laws for tasks like controlling the shape of a image curve or tracking a given curve. Our study indicates that the shape of the image curve is controllable only up to its linear curvature terms (in the 2-D case). However, there exist state feedback control laws (using only “up to curvature” terms) enabling the mobile robot to track arbitrary analytic curves. Such control laws are not necessarily the only ones. In applications, other control laws may be designed and used to obtain better control performances.

Generally speaking, there are two basic ways to use information from vision sensors for control purposes: using vision sensors to provide environmental information for higher level decisions (so called open-loop planning); or using them directly in the feedback control loop as servoing sensors. As we show in Section IV-B2 (Tracking Arbitrary Curves), the understanding of the image dynamics can also help to design appropriate open-loop control when the vision sensor does not provide enough information for applying feedback control.

In the cases that one has to approximate a general curve (which has infinite-dimensional dynamics) by simpler models, it is crucial to use models with properties which are invariant under the Euclidean motion (so-called intrinsic properties). We propose that linear curvature curves are very good candidates for such models. In some sense, linear curvature curves are a third-order approximation for general curves, so are third-order B-splines used by Frezza and Picci [12]. However, the Extended Kalman Filters needed to estimate their parameters are 4-D and $(N+2)$ -dimensional respectively (where N is the number of output measurements). The two schemes therefore differ in their computational intensity.

We are aware of the extensive literature on vision based control in driving applications. The models and the control laws that we propose are more appropriate for mobile robot applications, where in typical indoor environments the ground plane assumption is satisfied, and kinematic models are appropriate. We are currently working on generalizing some of the

ideas presented in this paper to the context of dynamic models. Some of the work in this direction can be found in [19].

Although visual servoing for ground-based mobile robot navigation has been extensively studied, its applications in aerial robot navigation have not received much attention. In the aerial robot case, the motions are 3-D rigid body motions $SE(3)$ instead of $SE(2)$ for ground-based mobile robots. Intrinsically, a mathematical formulation of this problem can be addressed as follows:

Consider $\Gamma(s)$ to be a curve to be tracked in \mathbb{R}^3 . The way to track this curve is through a projection to the camera plane $\pi: \mathbb{R}^3 \rightarrow \mathbb{R}^2$, π is either an orthographic or perspective projection. Further, $g(t) \in SE(3)$ represents the position and orientation of the camera respect to the spatial coordinate frame. Thus the curve $\Lambda(s, t)$ in the image plane is

$$\Lambda(s, t) = \begin{bmatrix} \lambda_1(s, t) \\ \lambda_2(s, t) \end{bmatrix} = \pi \circ g(t) \circ \Gamma(s). \quad (58)$$

Given a mathematical model of the kinematics of the mobile robot

$$\dot{g} = f(g, u) \quad (59)$$

where $f(g, u): SE(3) \times \mathbb{R}^{n_i} \rightarrow T(SE(3))$ is a vector field on $SE(3)$. Conceptually, the kinematics can then be lifted to a dynamical system (a Riccati-type PDE)

$$\begin{bmatrix} \frac{\partial \lambda_1(s, t)}{\partial t} \\ \frac{\partial \lambda_2(s, t)}{\partial t} \end{bmatrix} = \pi \circ f(g, u) \circ \Gamma(s) \quad (60)$$

for the curve in the image plane. The results in this paper relate the controllability properties of (59) to the controllability properties of the new system (60) for the 2-D case. A study of the more general 3-D case is in progress with applications to autonomous helicopter or aircraft navigation.

ACKNOWLEDGMENT

The authors would like to thank Dr. S. Soatto for a formulation of this problem at the AI/Robotics/Vision Seminar, University of California at Berkeley, October 1996.

REFERENCES

- [1] B. K. Ghosh and E. P. Loucks, “A perspective theory for motion and shape estimation in machine vision,” *SIAM J. Contr. Optimizat.*, vol. 33, no. 5, pp. 1530–1559, Sept. 1995.
- [2] D. Heeger and A. Jepson, “Subspace methods for recovering rigid motion,” *Int. J. Comput. Vision*, vol. 7, no. 2, pp. 95–117, Jan. 1992.
- [3] S. Soatto, R. Frezza, and P. Perona, “Motion estimation via dynamic vision,” *IEEE Trans. Automat. Contr.*, vol. 41, pp. 393–413, Mar. 1996.
- [4] C. Tomasi and T. Kanade, “Shape and motion from image streams under orthography: A factorization method,” *Int. J. Comput. Vision*, vol. 9, no. 2, Nov. 1992.
- [5] E. D. Dickmanns and V. Graefe, “Applications of dynamic monocular machine vision,” *Mach. Vision Appl.*, vol. 1, no. 4, pp. 241–261, 1988.
- [6] ———, “Dynamic monocular machine vision,” *Mach. Vision Appl.*, vol. 1, no. 4, pp. 223–240, 1988.
- [7] E. D. Dickmanns and B. D. Mysliwetz, “Recursive 3-D road and relative ego-state estimation,” *IEEE Trans. Pattern Anal. Machine Intell.*, vol. 14, pp. 199–213, Feb. 1992.
- [8] D. Raviv and M. Herman, “A “nonreconstruction” approach for road following,” in *Intell. Robots Comput. Vision*, vol. 1608, pp. 2–12, 1992.
- [9] B. Espiau, F. Chaumette, and P. Rives, “A new approach to visual servoing in robotics,” *IEEE Trans. Robot. Automat.*, vol. 8, pp. 313–326, June 1992.

- [10] C. Samson, M. Le Borgne, and B. Espiau, *Robot Control: The Task Function Approach*. Oxford, U.K.: Clarendon, 1991.
- [11] R. Pissard-Gibollet and P. Rives, "Applying visual servoing techniques to control a mobile hand-eye system," in *Proc. IEEE Int. Conf. Robot. Automat.*, Nagoya, Japan, May 1995, vol. 1, pp. 166–171.
- [12] R. Frezza and G. Picci, "On line path following by recursive spline updating," in *Proc. 34th IEEE Conf. Decision Contr.*, 1995, vol. 4, pp. 4047–4052.
- [13] S. Soatto, R. Frezza, and P. Perona, "Visual navigation by controlling apparent shape," *UC Berkeley AI/Robotics/Vision Seminar Notes*, Oct. 1996.
- [14] R. M. Murray, Z. Li, and S. S. Sastry, *A Mathematical Introduction to Robotic Manipulation*. Boca Raton, FL: CRC, 1994.
- [15] R. M. Murray and S. S. Sastry, "Nonholonomic motion planning: Steering using sinusoids," *IEEE Trans. Automat. Contr.*, vol. 38, pp. 700–716, May 1993.
- [16] J. Hauser and R. Hindman, "Maneuver regulation from trajectory tracking: Feedback linearization systems," *Post-print Vol. 3rd IFAC Symp. Proc. IFAC Symp. Nonlinear Contr. Syst. Design*, 1996, vol. 2, pp. 595–600.
- [17] G. Walsh, D. Tilbury, S. Sastry, R. Murray, and J. P. Laumond, "Stabilization of trajectories for systems with nonholonomic constraints," *IEEE Trans. Automat. Contr.*, vol. 39, pp. 216–222, Jan. 1994.
- [18] Y. Ma, J. Košecká, and S. Sastry, "Vision guided navigation of a nonholonomic mobile robot," *UC Berkeley Memo.*, vol. UCB/ERL, no. M97/34, 1997.
- [19] J. Košecká, R. Blasi, C. J. Taylor, and J. Malik, "Vision-based lateral control of vehicles," in *Proc. Intell. Transportation Syst. Conf.*, Boston, MA, 1997.
- [20] R. W. Brockett, R. S. Millman, and H. J. Sussmann, *Differential Geometric Control Theory*. Boston, MA: Birkhauser, 1983.
- [21] J. Weber, D. Koller, Q. T. Luong, and J. Malik, "An integrated stereo-based approach to automatic vehicle guidance," in *Proc. IEEE Int. Conf. Comput. Vision*, June 1995, pp. 52–57.
- [22] D. Tsakiris, C. Samson, and P. Rives, "Vision-based time-varying mobile robot control," in *Proc. Res. Workshop ERNET*, 1996, pp. 163–72.
- [23] D. Tilbury, R. Murray, and S. Sastry, "Trajectory generation for the n-trailer problem using Goursat Normal Form," *IEEE Trans. Automat. Contr.*, vol. 40, pp. 802–819, May 1995.
- [24] R. M. Murray, "Nilpotent bases for a class of nonintegrable distributions with applications to trajectory generation for nonholonomic systems," Tech. Rep. CIT/CDS 92-002, California Inst. Technol., Pasadena, CA, Oct. 1992.
- [25] J. P. Hespanha and A. S. Morse, Personal communication, May 1998.
- [26] A. Isidori, *Nonlinear Control Systems, Communications and Control Engineering Series*. New York: Springer-Verlag, 1989, 2nd ed.
- [27] S. Sastry, *Nonlinear Systems: Analysis, Stability and Control*. Reading, MA: Addison Wesley, 1999.
- [28] S. Soatto and P. Perona, "Recursive estimation of camera motion from uncalibrated image sequences," in *Proc. ICIP-94*, Nov. 1994, vol. 3, pp. 58–62.
- [29] A. H. Jazwinski, *Stochastic Processes and Filtering Theory*. New York: Academic, 1970.
- [30] J. M. Mendel, *Lessons in Digital Estimation Theory*. Englewood Cliffs, NJ: Prentice-Hall, 1987.
- [31] R. Cipolla and A. Blake, "Surface orientation and time to contact from image divergence and deformation," in *Proc. 2nd Eur. Conf. Comput. Vision*, May 1992, pp. 187–202.



Jana Košecká received the M.S.E.E. degree in electrical engineering and computer science from Slovak Technical University, Bratislava, Slovakia, in 1988, and the M.S. and Ph.D. degrees in computer science from the University of Pennsylvania, Philadelphia, in 1992 and 1996, respectively.

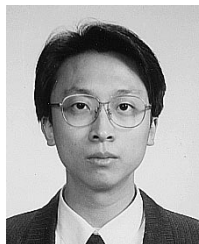
She is a Research Engineer at the Department of Electrical Engineering and Computer Science, University of California, Berkeley. Her research interests include computer vision, with emphasis on to visual servoing and control, structure, and motion recovery and self-calibration from image sequences. She is also interested in control and sensing for distributed multiagent systems, with applications to mobile robotics, unmanned aerial vehicles, autonomous car driving, and air-traffic management systems.



Shankar S. Sastry (F'95) received the Ph.D. degree from the University of California, Berkeley (UC Berkeley), in 1981.

He was on the faculty of the Massachusetts Institute of Technology (MIT), Cambridge, from 1980 to 1982 and Harvard University, Cambridge, as a Gordon McKay Professor in 1994. He is a Professor of electrical engineering and computer sciences and Director of the Electronics Research Laboratory, UC Berkeley. He has held visiting appointments at the Australian National University, Canberra, the University of Rome, Scuola Normale, Italy, and University of Pisa, Italy, the CNRS laboratory LAAS, in Toulouse, France, and as a Vinton Hayes Visiting fellow at the Center for Intelligent Control Systems, MIT. His areas of research are nonlinear and adaptive control, robotic telesurgery, control of hybrid systems, and biological motor control. He is a coauthor of *Adaptive Control: Stability, Convergence and Robustness* (Englewood Cliffs, NJ: Prentice Hall, 1989), and *A Mathematical Introduction to Robotic Manipulation* (Boca Raton, FL: CRC, 1994). His book *Nonlinear Control: Analysis, Stability and Control* is to be published by Springer-Verlag in 1999. He has co-edited *Hybrid Control II*, *Hybrid Control IV*, *Hybrid Systems: Computation and Control*, and *Springer Lecture Notes in Computer Science* in 1995, 1997, and 1998.

Dr. Sastry was an Associate Editor of the IEEE TRANSACTIONS ON AUTOMATIC CONTROL, IEEE CONTROL MAGAZINE, IEEE TRANSACTIONS ON CIRCUITS AND SYSTEMS, and the *Journal of Mathematical Systems, Estimation and Control* and is an Associate Editor of the *IMA Journal of Control and Information*, *The International Journal of Adaptive Control and Signal Processing*, and the *Journal of Biomimetic Systems and Materials*.



Yi Ma (S'98) received the B.S. degree in automatic control and the B.S. degree in applied mathematics, both from Tsinghua University, China, in 1995 and the M.S. degree in electrical engineering and computer science from the University of California, Berkeley in 1997, where he is currently pursuing the M.A. degree in mathematics and the Ph.D. degree in electrical engineering. His Ph.D. project is about both a differential geometric and a estimation theoretic approaches to multiview geometry, especially for motion and structure estimation from image

sequences.

His research interests include geometric control theory, multiview geometry in computer vision, visual servoing, and applications of differential geometry in system theory.